



HAL
open science

Transfer of polyglutamine aggregates in neuronal cells occurs in tunneling nanotubes.

Maddalena Costanzo, Saïda Abounit, Ludovica Marzo, Anne Danckaert, Zeina Chamoun, Pascal Roux, Chiara Zurzolo

► **To cite this version:**

Maddalena Costanzo, Saïda Abounit, Ludovica Marzo, Anne Danckaert, Zeina Chamoun, et al.. Transfer of polyglutamine aggregates in neuronal cells occurs in tunneling nanotubes.. Journal of Cell Science, 2013, 126 (16), pp.3678-85. 10.1242/jcs.126086 . pasteur-00874692

HAL Id: pasteur-00874692

<https://pasteur.hal.science/pasteur-00874692>

Submitted on 18 Oct 2013

HAL is a multi-disciplinary open access archive for the deposit and dissemination of scientific research documents, whether they are published or not. The documents may come from teaching and research institutions in France or abroad, or from public or private research centers.

L'archive ouverte pluridisciplinaire **HAL**, est destinée au dépôt et à la diffusion de documents scientifiques de niveau recherche, publiés ou non, émanant des établissements d'enseignement et de recherche français ou étrangers, des laboratoires publics ou privés.

Transfer of polyglutamine aggregates in neuronal cells occurs in tunneling nanotubes

Maddalena Costanzo¹, Saïda Abounit¹, Ludovica Marzo^{1,2}, Anne Danckaert³, Zeina Chamoun¹, Pascal Roux³ and Chiara Zurzolo^{1,2,*}

¹Institut Pasteur, Unité de trafic membranaire et pathogénèse, 28 rue du Docteur Roux 75724 Paris, Cedex 15, France

²Dipartimento di Biologia e Patologia Cellulare e Molecolare, Università Federico II, Napoli, Italy

³Institut Pasteur, Imagerie Dynamique, Plate-forme d'Imagerie Dynamique, 28 rue du Docteur Roux 75724 Paris, Cedex 15, France

*Author for correspondence (chiara.zurzolo@pasteur.fr)

Accepted 28 May 2013

Journal of Cell Science 126, 3678–3685

© 2013. Published by The Company of Biologists Ltd

doi: 10.1242/jcs.126086

Summary

Huntington's disease (HD) is a dominantly inherited neurodegenerative disease caused by CAG expansion in the huntingtin gene, which adds a homopolymeric tract of polyglutamine (polyQ) to the encoded protein leading to the formation of toxic aggregates. Despite rapidly accumulating evidences supporting a role for intercellular transmission of protein aggregates, little is known about whether and how huntingtin (Htt) misfolding progresses through the brain. It has been recently reported that synthetic polyQ peptides and recombinant fragments of mutant Htt are readily internalized in cell cultures and able to seed polymerization of a reporter wild-type Htt. However, there is no direct evidence of aggregate transfer between cells and the mechanism has not been explored. By expressing recombinant fragments of mutant Htt in neuronal cells and in primary neurons, we found that aggregated fragments formed within one cell spontaneously transfer to neighbors in cell culture. We demonstrate that the intercellular spreading of the aggregates requires cell–cell contact and does not occur upon aggregate secretion. Interestingly, we found that the expression of mutant, but not wild-type Htt fragments, increases the number of tunneling nanotubes, which in turn provide an efficient mechanism of transfer.

Key words: Protein misfolding, HTT, Intercellular transfer

Introduction

Huntington's disease (HD) is an autosomal dominant neurodegenerative disorder caused by the expansion of a CAG repeat in the exon 1 of the huntingtin gene. The resulting huntingtin protein (Htt) includes a toxic expanded polyglutamine (polyQ) stretch causing its misfolding and subsequent aggregation (Davies et al., 1997; DiFiglia et al., 1997).

HD is characterized by a cortical degeneration that follows a topologically predictable pattern (Rosas et al., 2008) and precedes degeneration in the striatum (Brundin et al., 2010; Vonsattel and DiFiglia, 1998). A progression which begins in a specific area of the brain and extends along predictable anatomical paths (Brundin et al., 2010) is characteristic of protein conformational neurodegenerative disorders, including Alzheimer's, Parkinson's and prion diseases (Carrell and Lomas, 1997). Numerous studies suggest that in these disorders, disease-associated protein aggregates can transfer between cells contributing to the anatomical spreading of the underlying pathology, similar to infectious prions (Brundin et al., 2010; Lee et al., 2010; Costanzo and Zurzolo, 2013).

In HD studies, synthetic polyQ peptides and recombinant fragments of mutant Htt applied to cultured cells are readily taken up (Ren et al., 2009; Yang et al., 2002) and access the cytoplasm where they can seed polymerization of a soluble Htt reporter (Ren et al., 2009). These assemblies persist for over 80 generations in prolonged cell culture despite their dilution in dividing cells, suggesting a self-sustaining seeding and fragmentation process reminiscent of prion replication (Ren

et al., 2009; reviewed by Polymenidou and Cleveland, 2012). However, cell-to-cell transmission of Htt was inefficient in co-culture of non-neuronal cells (Ren et al., 2009).

Seeding of intracellular protein aggregates by external amyloid fibrils have been shown in a cell culture model for tau aggregation (Guo and Lee, 2011; Nonaka et al., 2010). Furthermore, spontaneously formed aggregates were also able to transfer between cells (Frost et al., 2009). The uptake of extracellular aggregates containing tau (Frost et al., 2009; Kfoury et al., 2012; Wu et al., 2013) or α -synuclein (Angot et al., 2012; Danzer et al., 2009; Hansen et al., 2011; Konno et al., 2012; Luk et al., 2009; Nonaka et al., 2010; Volpicelli-Daley et al., 2011; Waxman and Giasson, 2010) resulted in their delivery to the endocytic compartment from which they escape to nucleate aggregation of endogenous cytosolic proteins. Alternatively prions and amyloid- β were shown to transfer between cells via tunneling nanotubes (TNTs) (Gousset et al., 2009; Wang et al., 2011). These are thin actin-rich membrane bridges connecting the cytoplasm of distant cells (Rustom et al., 2004) and allowing exchange of cellular components between cells. Vesicles derived from various organelles (early endosomes, endoplasmic reticulum, Golgi complex and lysosome), plasma membrane components, cytoplasmic molecules, ions, as well as pathogens have been shown to travel through TNTs (Abounit and Zurzolo, 2012; Marzo et al., 2012). Therefore, it is possible that TNTs could be hijacked by other 'prion-like' protein aggregates. In the present study we investigated the capacity of intracellular aggregates of a mutant Htt fragment to transfer

between co-cultured neuronal cells as well as in primary neurons. Using both flow cytometry and microscopy approaches, we found that upon expression of Htt mutant fragments in neuronal cells as well as in primary neurons, aggregates were spontaneously transferred to neighboring cells. Differently from previous data, we demonstrate that this transfer is quite efficient and does not rely on release from dying cells as a result of mutant Htt-induced toxicity (Ren et al., 2009; Saudou et al., 1998). We also show that transfer does not occur through the supernatant but requires cell-to-cell contact. Of interest, aggregates were found in TNTs, which were increased by the expression of mutant Htt fragments. Therefore, TNTs could provide an efficient mechanism of transfer of polyQ aggregates between neuronal cells.

Results

Intracellular mutant Htt aggregates transfer between co-cultured CAD cells

The first 480 amino acids of Htt containing either 17Q (wild-type 480-17Q) or 68Q repeats (mutant 480-68Q) fused to green fluorescent protein (GFP-480-17Q and GFP-480-68Q, respectively) were expressed in CAD neuronal cells (Fig. 1A). These N-terminal fragments of Htt have been shown to retain the property of the full length protein regarding both aggregation and toxicity and have been used as robust models of Huntington's pathology both *in vitro* and *in vivo* (Bjørkøy et al., 2005; Mangiarini et al., 1996; Saudou et al., 1998; Zala et al., 2008).

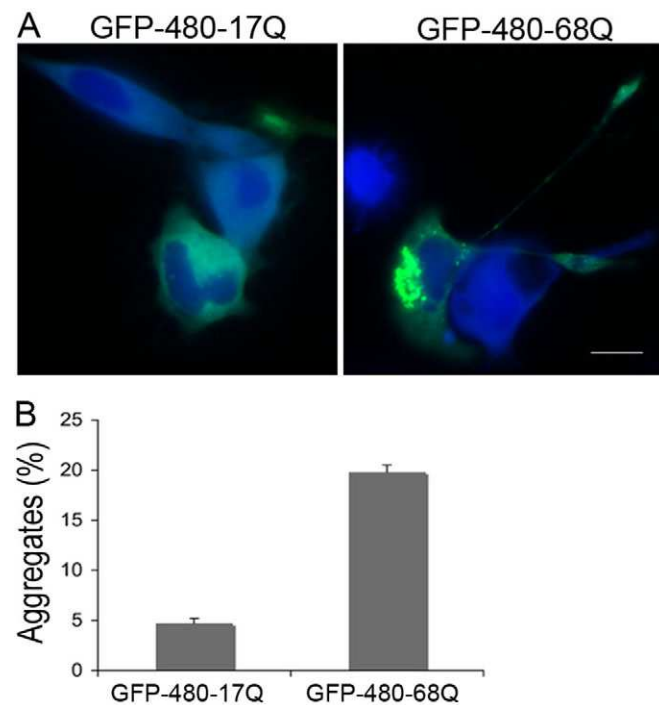


Fig. 1. GFP-480-68Q overexpression in CAD cells leads to aggregate formation. (A) 48 hours after transfection with GFP-480-17Q or GFP-480-68Q constructs, CAD cells were stained with HCS CellMask™ Blue to label the cytosol. Images are representative of three independent experiments. Scale bar: 10 μ m. (B) Quantification of the number of fluorescent aggregates, based on manual counting, in transfected cells. After 48 hours \approx 4.9% of cells have spontaneous aggregation of GFP-480-17Q compared with \approx 23% of GFP-480-68Q-expressing cells ($n=3$, 100 transfected cells counted per experiment). Values are means \pm s.e.m.

Aggregate-containing cells were quantified 48 hours post-transfection. 23% of the cells expressing GFP-480-68Q contained aggregates, while less than 5% of GFP-480-17Q cells showed diffuse nucleocytoplasmic fluorescence with GFP puncta (Fig. 1B).

In order to understand whether intracellular Htt aggregates were able to transfer between co-cultured cells, we set up a flow cytometry assay. CAD cells were transfected with either GFP-480-68Q (donor) or with mCherry (acceptor). 1 day post-transfection, the two cell populations were co-cultured at a ratio 1:1 for 24 hours prior to flow cytometry (see Materials and Methods). As control for the background signal, donor and acceptor cells were cultured separately for 24 hours and mixed immediately before flow cytometry. 3.7% of acceptor cells co-cultured with GFP-480-68Q cells scored as GFP/mCherry double positive while only 0.5% of acceptor cells were double positive when the two populations were mixed prior to flow cytometry (i.e. background, mix) (Fig. 2A,B).

These data were confirmed by fluorescence microscopy since we observed the presence of GFP-480-68Q aggregates in almost 4% of mCherry acceptor cells after 24 hours of co-culture (Fig. 2C).

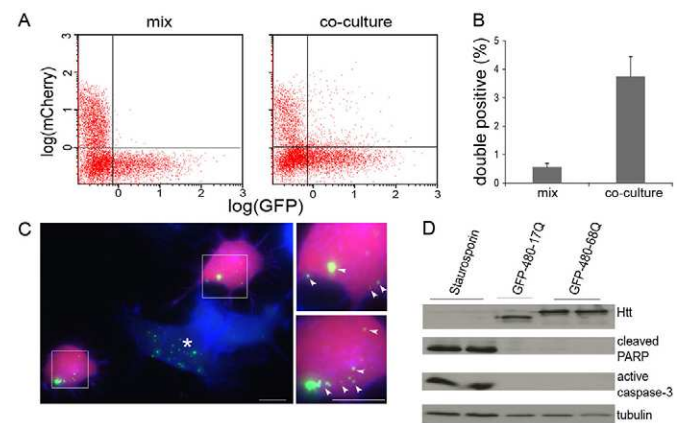


Fig. 2. GFP-480-68Q aggregates transfer between co-cultured CAD cells. (A) Cells were separately transfected with either GFP-480-68Q (donor) or mCherry (acceptor) constructs for 24 hours. The two cell populations were either mixed immediately prior to analysis (mix) or co-cultured for additional 24 hours (co-culture). Flow cytometry was used to quantify the percentage of acceptor cells containing aggregates. Representative cell plot are shown. (B) Quantification of flow cytometry experiment revealed that 0.5% of cell scored positive for both GFP and mCherry fluorescence (upper right quadrant of the cell plot) when they were mixed just before analysis, whereas 3.7% of cells scored double positive when co-cultured for 24 hours prior to the analysis, indicating transfer of GFP-480-68Q aggregates ($n=3$, 10,000 cells recorded per condition in each experiment). (C) One-day post-transfection GFP-480-68Q and mCherry cells were co-cultured on Ibidi® dishes for 24 hours. Cells were then fixed and stained with HCS CellMask™ to label the cytosol. Multiple GFP-480-68Q aggregates (insets, white arrowheads) are visible within mCherry cells, confirming transfer of GFP-480-68Q aggregates. A GFP-480-68Q-transfected cell with aggregates is indicated with an asterisk. Scale bars: 10 μ m. (D) GFP-480-17Q GFP-480-68Q cells were lysed 48 hours after transfection. Whole-cell extracts were prepared, separated by SDS-PAGE gel and analyzed by western blotting using antibodies against cleaved PARP and active caspase-3. Anti-tubulin shows equal loading. Results are representative of three independent experiments. Activation of apoptosis in GFP-480-68Q cells was not detected in comparison to control GFP-480-17Q cells.

Because GFP-480-68Q has been shown to induce cell death in neuronal cell culture (Bjørkøy et al., 2005; Saudou et al., 1998), aggregate transfer could derive from the internalization into recipient cells of Htt aggregates released in the medium from dying cells as it was previously suggested (Ren et al., 2009). To test this possibility, we monitored cell death in GFP-480-68Q-transfected cells compared to control cells transfected with GFP-480-17Q at 48 hours post-transfection corresponding to the time point of the transfer experiments (see above). We analyzed by western blotting both active caspase-3 and cleaved PARP as markers of apoptosis (Fig. 2D) and assessed DNA fragmentation by TUNEL (TdT-mediated dUTP nick-end labeling) using fluorescence microscopy, to monitor apoptosis and necrosis (data not shown). To be sure to include dead/dying cells that might have detached from the dishes we also quantify cell death by flow cytometry of floating and adherent cells after staining with propidium iodide (see Materials and Methods; supplementary material Fig. S1A). While there was no difference in the cell death of adherent cells (less than 1%) between control and transfected cells, the FACS analysis showed a negligible number of floating cells in all sample (supplementary material Fig. S1B). Thus with these combined approaches we could not detect any induction of cell death in CAD cells expressing either GFP-480-68Q or GFP-480-17Q. Overall, these data indicate that at 48 hours post-transfection, aggregates formed within a cell are able to transfer to acceptor cells through a process that is independent of their release due to cell death.

Intercellular transfer of Htt aggregates requires cell–cell contact

The transfer of Htt aggregates could have occurred either through cell–cell contact or secretion in the extracellular space (i.e. in the culture media). Therefore, we examined whether Htt aggregates transfer would occur between cells separated by filters, which would allow the passage of secretory vesicles and exosomes but would not allow cell-to-cell contact. To this aim, 1-day post-transfection, GFP-480-68Q donor cells were plated on filters positioned in a plate on top of a layer of acceptor cells expressing mCherry and incubated for 24 hours (see Materials and Methods). Under these conditions only 0.18% of acceptor cells were scored as GFP/mCherry double positives by flow cytometry analysis (Fig. 3), showing that the transfer efficiency was reduced by more than 95% (to the background levels) when filters were used to separate the two populations compared to direct co-cultures.

These results suggest that in our experimental conditions secretion is not the predominant mode of passage of aggregates between neuronal cells. However, to rule out the possibility that filters could trap Htt aggregates, we analyzed whether transfer was mediated by the supernatant of GFP-480-68Q cells that would have released GFP-480-68Q aggregates in the culture medium. To this aim at 1-day post-transfection the medium of mCherry cells was replaced with the supernatant of GFP-480-68Q cells collected at 48 hours post-transfection. Then, after 24 hours of exposure to the conditioned medium, mCherry cells were analyzed by flow cytometry and scored for the presence of Htt aggregates. Similarly to what we observed in the filter experiments, only 0.04% of mCherry cells scored as double positives, further confirming that at early times post-infection (48 hours), secretion into the medium is not the main transfer mechanism of Htt aggregates (Fig. 3).

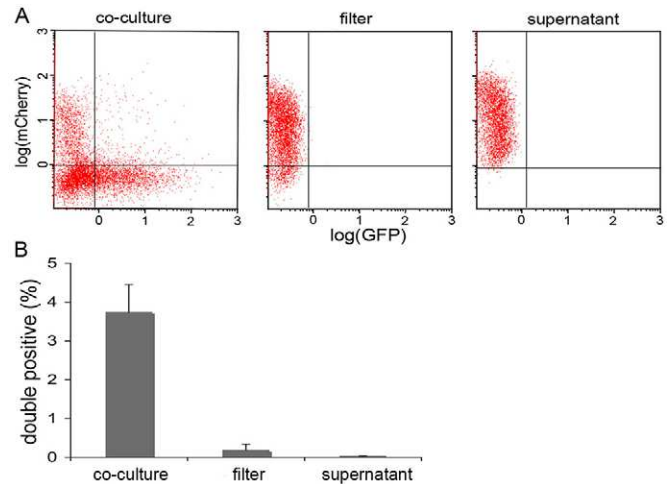


Fig. 3. Cell-to-cell contact is required for GFP-480-Q68 aggregate transfer in CAD cells. To determine the impact of GFP-480-68Q aggregates present in the supernatant (e.g. exosomal release, vesicle secretion), cells were separately transfected with either GFP-480-68Q or mCherry. The day after, mCherry cells were co-cultured with GFP-480-68Q cells directly (co-culture) or through filters (filter) or exposed to the 24-hours-conditioned medium of GFP-480-68Q cells (supernatant) for an additional 24 hours. Flow cytometry was used to quantify double positive cells. Representative cell plot are shown. (B) Quantification of flow cytometry experiments revealed only 0.18% and 0.04% of cells scored positive for both GFP and mCherry fluorescence in filter and supernatant condition, respectively. These data indicate that an efficient transfer (3.7% of GFP/mCherry double positive cells) is occurring only when direct cell-to-cell contact is allowed (means \pm s.e.m., $n=3$, 10,000 cells recorded per condition in each experiment).

Tunneling nanotubes mediate intercellular transfer of Htt aggregates in CAD cells

Overall the above data indicate that cell-cell contact is required for cell-to-cell transfer of intracellular Htt aggregates. One attractive possibility is that Htt aggregates formed within one cell might access the cytoplasm of neighboring uninfected cells by hijacking Tunneling Nanotubes (TNTs) (Abounit and Zurzolo, 2012; Marzo et al., 2012), as it was previously shown for PrP^{Sc} (Gousset et al., 2009) and amyloid- β particles (Wang et al., 2011). To evaluate this possibility, CAD cells expressing either GFP-480-68Q or mCherry were co-cultured 24 hours post-transfection on plastic bottom dishes ready for imaging (Ibidi®) in a well-spaced manner to favor the formation of TNTs, as previously shown (Gousset et al., 2009). After 24 hours of co-culture (48 hours post-transfection, same as for the flow cytometry analyses) cells were fixed, and stained with WGA–Alexa Fluor® conjugate to label TNT membranes in non permeabilized condition. By fluorescence microscopy we could visualize a relevant percentage (42%) of mCherry cells containing multiple GFP aggregates connected to GFP-480-68Q cells through TNTs, which was suggestive of a role of these structures in aggregate transfer. However, we could not detect GFP-480-68Q aggregates inside TNTs. This could indicate that transfer of aggregates through TNTs had already occurred at the time of cell fixation. In order to test this hypothesis, we repeated the same experiment by co-culturing the two cell populations for shorter time (12 hours which corresponds to 36 hours post-transfection). Under these conditions, we could detect GFP-480-68Q aggregates within TNTs connecting distant cells (Fig. 4A,

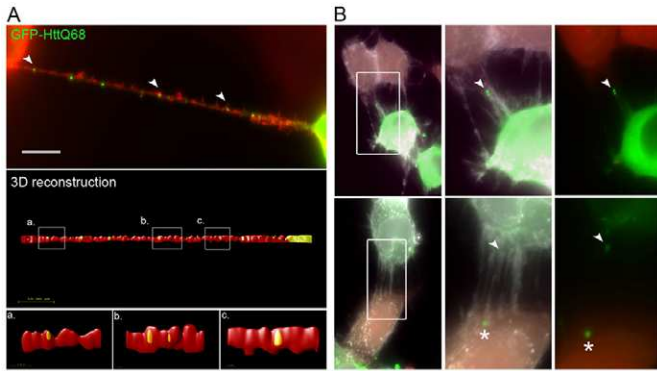


Fig. 4. Transfer of GFP-480-68Q aggregates occurs through TNTs in co-cultured CAD cells. 1-day post-transfection, GFP-480-68Q-transfected cells (donor, green) and mCherry-transfected cells (acceptor, red) were co-cultured on Ibidi® dishes and fixed after 12 hours (36 hours post-transfection). Cells were stained with WGA–Alexa Fluor®–Rhodamine (red in A) or Alexa Fluor® 350 conjugate (white in B) to label TNTs. (A) GFP-480-68Q aggregates were found inside TNTs connecting distant cells (white arrowheads top panel and insets a, b, c). The wide-field image is shown in the top panel. The TNT structure is labeled in red with WGA–Rhodamine and GFP-480-68Q aggregates (arrowheads) appears either green or yellow. After performing three-dimensional reconstruction using Huygens Essential software, aggregates are yellow, indicating that they are present within the lumen of the TNT (second middle panel and insets). Insets a, b and c show enlarged views of the boxed areas; aggregates are clearly present within the lumen of the TNT. (B) GFP-480-68Q aggregates were found inside TNTs connecting GFP-480-68Q/mCherry cell pairs (white arrowheads), as well as in the cytoplasm of mCherry cells (white asterisks) suggesting TNT-mediated transfer of GFP-480-68Q aggregates between the two cell populations. The boxed areas are magnified on the right. In the third panel the white channel has been removed to better visualize the GFP-480-68Q aggregates (arrowheads and asterisks). Images are representative of three independent experiments and were obtained in non-permeabilized conditions. Scale bars: 10 μ m.

top panel) and between the two different cell populations (GFP-480-68Q/mCherry cell pairs; Fig. 4B, top panel). Deconvolution of the images prior to three-dimensional reconstruction using the Huygens Professional and Huygens Essential softwares allowed us to further confirm that the aggregates are inside the TNTs and not on the outside (Fig. 4A). Furthermore, we found GFP-480-68Q aggregates in the lumen of TNT-paired mCherry cells, supporting TNT-mediated transfer (Fig. 4B and inset).

Because we failed to detect aggregates in TNTs at later time points (i.e. 48 hours post-transfection) these data suggested a relationship between time after transfection and transport along TNTs. Therefore, we decided to further characterize the Htt aggregates in our cell culture over time. By using the Huygens Professional software upon deconvolution of wide-field images, we quantified both the number and the size of the aggregates at 24 hours, 36 hours and 48 hours post-transfection. We found that while the number of aggregates per cell progressively decreases over time (from 8.1 at 24 hours to 6.7 at 36 hours to 2.4 at 48 hours), their size (defined as percent of the cell volume) significantly increases between 36 hours and 48 hours (from 1.4% to 8.7%, respectively; supplementary material Fig. S2). Furthermore, we observed that aggregates are sparse in the cytoplasm at 24 and 36 hours post-transfection while they appear more concentrated in perinuclear position at 48 hours post-transfection. Overall, these data indicate that transfer through

TNTs is an early event that might provide an efficient mechanism for the spreading of early forming aggregates between cells. Because the aggregate size increases progressively with time in cell culture this may explain why we do not observe aggregates in TNTs at later time points.

Next, in order to better characterize this transfer mechanism, we quantified the occurrence of TNTs in GFP-480-68Q cells compared to control cells transfected with wild-type GFP-480-17Q or GFP vector at different time points in culture. 12 hours post-transfection the cells were detached and replated on Ibidi® dish. Then, they were fixed 12 or 24 hours after replating, corresponding to 24 and 48 hours post-transfection. Labeling with wheat germ agglutinin (WGA)–Rhodamine and HCS CellMask™ Blue allowed the detection of TNT structures and cell bodies respectively (Fig. 5A). Interestingly, we found that 48 hours post-transfection the GFP-480-68Q cell population, displayed a 20% increase of TNT-connected cells compared to the control GFP-480-17Q or GFP populations (Fig. 5B). These data indicate that the expression of GFP-480-68Q increases TNT connections between cells, which in turn could facilitate the intercellular spreading of Htt aggregates.

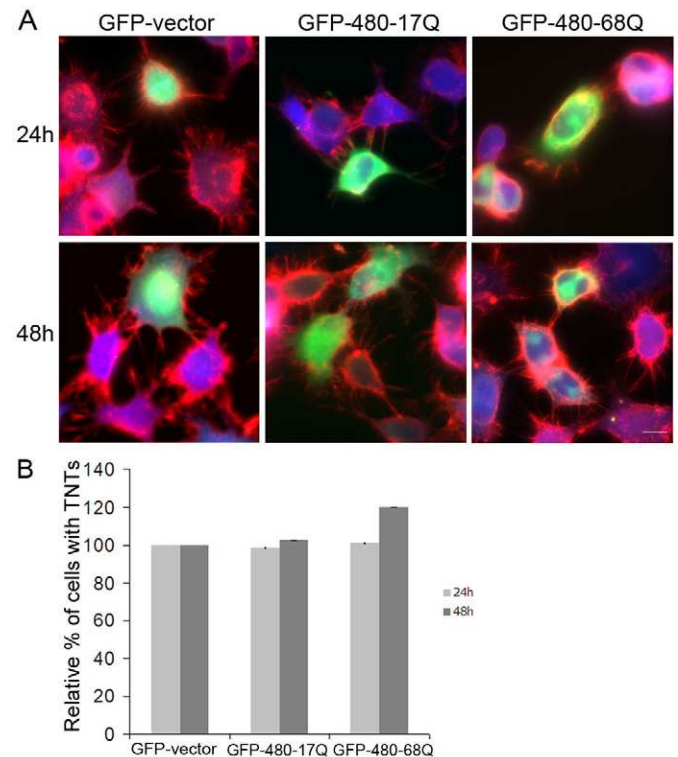


Fig. 5. Overexpression of GFP-480-68Q but not GFP-480-17Q in CAD cells increases TNT number. (A) CAD cells were transfected with GFP, GFP-480-17Q or GFP-480-68Q. To ensure the optimal cell density for TNT formation, cells were detached after 12 hours and plated on Ibidi® dishes. The cells were then fixed 12 or 24 hours after plating (corresponding to 24 and 48 hours post-transfection, respectively) and labeled with WGA–Rhodamine (in red) and HCS cell mask (in blue) to detect both TNT structures and the cell body. Scale bar: 10 μ m. (B) Percentage of TNT-connected cells upon GFP-480-17Q or GFP-480-68Q overexpression relative to that of GFP-transfected cells as control (mean \pm s.e.m., $n=3$ independent experiments, 100 transfected cells per experiment).

Cell-to-cell transfer of mutant Htt aggregates occurs in primary neurons and requires intercellular contact

Having demonstrated that transfer of intracellular Htt aggregates occurs between CAD cells, we further investigated their ability to transfer between primary neurons. To this aim, we established *in vitro* co-cultures of primary Cerebellar Granule Neurons (CGNs). Specifically, GFP-480-68Q- and mCherry-transfected CGNs were plated on coverslips at a ratio 1:1.5 respectively and incubated for 140 hours before fixation (see Materials and Methods). Cells were immunolabeled with an anti-Htt antibody that recognizes both endogenous Htt and the transfected mutant fragment. Mosaics of different fields were generated by wide-field microscopy (Zeiss Axiovert 200M) to analyze the overall neuronal network. We could detect aggregates of GFP-480-68Q in mCherry neurons both in neurites and in the cell body around the nucleus (Fig. 6). Quantification of the transfer events by using a dedicated version of the AcapellaTM software (Perkin-Elmer; see Materials and Methods) revealed that about 4% of mCherry neurons contained GFP-480-68Q aggregates. To our knowledge, this is the first evidence that Htt aggregates formed within one neuron can transfer to non-transfected cells in primary cultures.

In primary neurons cell-to-cell transmission of cytosolic aggregates could occur either through their release in the

extracellular space (endo/exocytosis, exosomes, trans-synaptic transmission at axonal terminals) or through direct passage from the cytosol of one neuron to the other, possibly via TNTs (Marzo et al., 2012; Moreno-Gonzalez and Soto, 2011). To evaluate the possible role of the secretory pathway in the interneuronal transfer, we plated GFP-480-68Q- and mCherry-transfected CGNs on separated coverslips in the same dish, thus, impairing intercellular contact but allowing exchange between the two different populations through the medium. After 140 hours of incubation, neurons were washed, fixed and analyzed by wide-field microscopy (Fig. 6B). In this condition, we were not able to detect Htt aggregates in mCherry-labeled neurons, which suggests that cell-to-cell contact is required and that secretion is not the main transfer mechanism for mutant GFP-480-68Q aggregates in primary neuronal cultures. Interestingly, we found aggregates in TNT-like connections between neurons and astrocytes (data not shown), suggesting that TNTs have a role also in transfer between primary neurons, similar to neuronal cell lines.

Discussion

In the present study we have tested the hypothesis that Htt aggregates transfer between neuronal cells. We developed an *in vitro* approach in which CAD (mouse catecholaminergic neuronal cell line, Cath.a-Differentiated) cells expressing an expanded-polyglutamine fragment of huntingtin (GFP-480-68Q) prone to aggregation (Björkøy et al., 2005; Saudou et al., 1998; Zala et al., 2008) were co-cultured with acceptor cells expressing cytosolic mCherry. By flow cytometry analysis we found that after 24 hours of co-culture, 4% of the acceptor cells also exhibited GFP staining, which is a sign of GFP-480-68Q transfer. These results were further confirmed by wide-field microscopy, showing mCherry cells containing multiple GFP-positive aggregates in close proximity to GFP-480-68Q-expressing cells.

To our knowledge, this is the first direct demonstration that polyQ aggregates formed within a neuronal cell can efficiently transfer to neighboring cells. These data are in agreement with a previous report showing low rate of movement of mutant Htt (103Q^{Htt}-V1 and 103Q^{Htt}-V2 plasmids) by Bimolecular Fluorescence Complementation (Herrera et al., 2011). The transfer of Htt aggregates was also suggested by Ren and colleagues (Ren et al., 2009) which observed a modification of the staining pattern of a wild-type Htt reporter, from diffuse fluorescence to puncta, in non-neuronal cells (HEK293) when co-cultured with cells expressing an expanded-polyQ fragment (Ren et al., 2009). The precise colocalization of the reporter puncta with the polyQ aggregates indicated cell-to-cell transfer of aggregates, leading to the seeded polymerization of the soluble reporter; however, no direct evidence for aggregate transfer was provided. Moreover, the same study concluded that spontaneous transfer of polyQ aggregates was rather inefficient because the number of reporter cells with puncta could be markedly increased upon selective lysis of the donor cells (Ren et al., 2009), suggesting that aggregates were internalized upon passive release from dead or dying cells. Interestingly, in our conditions we could not detect cell death in GFP-480-68Q-transfected CAD cells 48 hours post-infection. This indicates that in our experimental conditions, aggregates transfer is an active mechanism that occurs efficiently between intact, viable neuronal cells at an early stage post-infection. To our

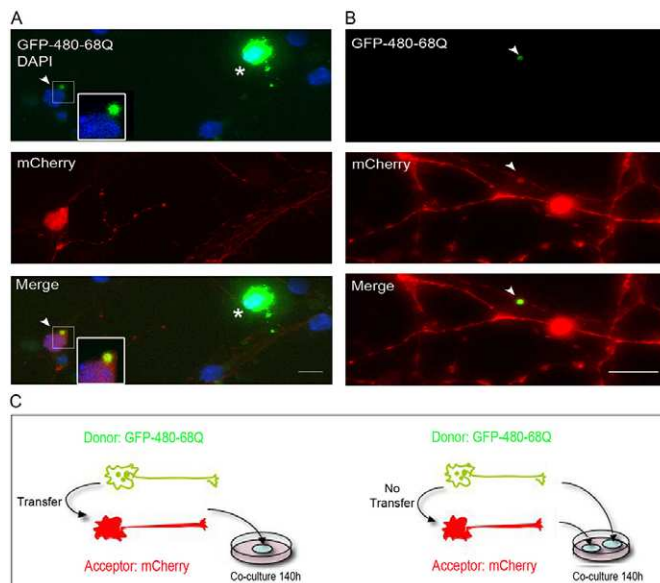


Fig. 6. GFP-480-68Q aggregates transfer between primary CGN co-cultures. Immediately after isolation, CGNs were transfected with either GFP-480-68Q (donor) or mCherry (acceptor) and co-cultured at a ratio 1:1.5 on coverslips for 140 hours. Cells were then washed, fixed and labeled with DAPI. Mosaics (3×3 fields) were acquired by wide-field microscopy to visualize the neuronal network. For acquisition, Z-stacks (0.4 μm) were taken. GFP-480-68Q aggregates (white arrowheads) were found both in the cell body (A) and in the neurites (B) of mCherry neurons, indicating cell-to-cell transfer of GFP-480-68Q aggregates in primary neuronal co-cultures. *A GFP-480-68Q cell containing aggregates. Insets in A show enlarged views of the boxed areas. Representative tiles of three independent experiments are shown. Scale bars: 10 μm. (C) Schematic representation of the co-culture experiments in primary CGNs. Only when donor and acceptor neurons were plated on the same coverslips, thus allowing intercellular contact, could we detect transfer of GFP-480-68Q aggregates to mCherry CGNs (acceptor neurons).

knowledge, this is the first direct demonstration that polyQ aggregates formed within a cell (and not exogenously added to the cell culture) transfer efficiently to neighboring cells.

To characterize the transfer mechanism we had to distinguish between direct cell-cell transfer, which requires cell contact, and transfer through the medium (e.g. following secretion of the aggregates). When cells were co-cultured through filters, the transfer efficiency was reduced to background noise compared to direct co-culture, arguing against secretion. Similar results were obtained when we exposed acceptor cells to the conditioned medium of GFP-480-Q68 cells ruling out the possibility that aggregates were retained on the filters.

Since in the pathogenesis of HD the target cells are post-mitotic neurons, we next characterized whether and how expanded-polyQ aggregates transferred between primary neurons. Consistent with the findings in CAD cells, we could detect cell-to-cell transfer of aggregates from primary neurons expressing GFP-480-68Q to mCherry-expressing neurons only when they were co-cultured on the same coverslips, but not when the two different populations only shared the medium (Fig. 6C).

Overall, these results indicate that in both neuronal cell cultures and primary neurons, direct cell-to-cell contact is required for efficient transfer of GFP-480-68Q aggregates, since no detectable transfer occurs by release/secretion of the aggregates in the medium in our culturing condition (e.g. 24 hours co-culture; 1:1 cell ratio). Furthermore, as Htt aggregates are either cytosolic or nuclear, transfer to neighboring cells through the plasma membrane by cell surface contact is not likely to occur.

By fluorescence microscopy and three-dimensional reconstruction of deconvolved images, we found that GFP-480-68Q aggregates were inside TNTs connecting two neuronal cells similarly to what was previously reported for infectious prions (Gousset et al., 2009) and for β -amyloid (Wang et al., 2011). We also found aggregates in TNT-like connections between neurons and astrocytes (data not shown), suggesting that TNTs have a role also in transfer between primary neurons, similar to neuronal cell lines. However the lack of specific marker impairs the unequivocal identification of TNTs in primary neurons. Interestingly Htt aggregates were found in TNTs upon 12 hours of co-culture of CAD cells (corresponding to 36 hours post-transfection), whereas 24 hours after co-culture (48 hours post-transfection) we could visualize multiple Htt aggregates inside the acceptor cells but not in TNTs connecting the donor/acceptor populations. The mechanisms that regulate transfer through TNT structures are not fully understood and pathogens have been shown to hijack these structures (Abounit and Zurzolo, 2012; Marzo et al., 2012). As reported in a previous study (Shin et al., 2005), we observed that the size of the aggregates in cultured CAD cells increases with time from relatively sparse and smaller aggregates at 24 hours post-transfection to bigger ones concentrated in perinuclear positions at 48 hours post-transfection (supplementary material Fig. S2A,B), possibly due to the progressive nucleation of Htt molecules. Therefore, we hypothesize that transfer of aggregates occurs at early times after the establishment of the co-culture, and that the progressive increase in the aggregates size might impede their ability to hijack TNTs. In HD, deposition of protein aggregates is an early event in the pathogenic cascade and precedes neurodegeneration. Here we demonstrate that aggregate transfer occurs between intact, viable neuronal cells and could therefore contribute to the early stage of HD pathogenesis and to the progression of the

disease in the brain. In later stages, spreading of the aggregates upon their passive release from dead or dying cells, as suggested (Brundin et al., 2010; Ren et al., 2009), can also be envisaged and might further contribute to the progression of the disease.

Furthermore, upon overexpression of GFP-480-68Q (but not of the wild-type fragment GFP-480-17Q), we detected an increase in the number of TNT structures between CAD cells (Fig. 5A,B). Remarkably, this increase occurs between 24 and 48 hours post-transfection, which is consistent with the timing of aggregate detection in TNTs (36 hours post-transfection; Fig. 4). We hypothesize that the overexpression of the mutant fragment (but not of the wild-type one) constitutes a harmful insult to the cells leading to the activation of stress pathways and thus resulting in TNT induction, as recently proposed (Wang et al., 2011; Zhang, 2011). Overall, our results indicate that Htt aggregates hijack TNTs and that possibly the GFP-480-68Q fragment might indirectly increase TNT formation, thus optimizing aggregates transfer, similarly to what has been recently shown for HIV particles spreading (Eugenin et al., 2009). Because polyQ aggregates are cytosolic or nuclear, and do not appear to be associated with membrane vesicle (Ren et al., 2009) (supplementary material Fig. S3A) but are 'caged' by vimentin in aggresome-like structures (supplementary material Fig. S3B), a passage as aggresomes through TNTs can be envisaged. In addition, since Htt can interact with acidic phospholipids enriched on the cytoplasmic leaflet of the plasma membrane (Kegel et al., 2005; Kegel et al., 2009), a surfing process along the TNT membrane could also be possible (Marzo et al., 2012). Exploring the mechanisms by which cells form TNTs and transfer of material is regulated within these structures will be essential for a better understanding of the mechanisms of aggregate spreading. Further studies will be required to specifically address these questions.

As infectious prions, polyQ aggregates and possibly β -amyloid (Wang et al., 2011) transfer from cell-to-cell through TNTs, it is tempting to speculate that TNTs might constitute a general mechanism for the spreading of different β -sheet-enriched proteinaceous aggregates (Costanzo and Zurzolo, 2013; Marzo et al., 2012). The identification of specific TNTs markers *in vivo* will be critical to confirm their role in the progression of protein misfolding throughout brains undergoing neurodegenerative disorders (Costanzo and Zurzolo, 2013; Marzo et al., 2012).

Materials and Methods

Cell lines, mouse lines and primary cell cultures

CAD cells (mouse catecholaminergic neuronal cell line, Cath.a-Differentiated) were a gift of Dr Laude H. (Institut National de la Recherche Agronomique, Jouy-en-Josas, France) and were cultured in Opti-MEM (Gibco) with the addition of 10% FBS (fetal bovine serum). Primary cultures were established from C57BL/6J mice provided by Charles River Laboratories. All experiments were performed according to national guidelines.

Primary cultures of CGNs (cerebellar granule neurons) were established as previously described (Cronier et al., 2004; Langevin et al., 2010). CGNs were cultured for the indicated time on poly-D-lysine (10 μ g/ml; Sigma) pre-coated coverslips at a density of 400,000 cells/coverslip in DMEM (Dulbecco's modified essential medium; Gibco) supplemented with 10% (v/v) FBS, 20 mM KCl, penicillin (50 units/ml), streptomycin (50 μ g/ml; Gibco) and complemented with B27 and N2 supplement (Gibco).

All cultures were incubated at 37°C in a humidified atmosphere with 5% CO₂.

Plasmids and transfection procedures

GFP-480-68Q and GFP-480-17Q were a kind gift of Dr Humbert S. (Institut Curie – UMR 146 du CNRS, Centre Universitaire Orsay, France). mCherry vector was from Clontech.

CAD cells were transfected at 50% confluence with the indicated construct using Lipofectamine 2000 (Invitrogen), according to the producer's protocol.

CGNs were transfected with the appropriate construct in suspension immediately after isolation using the Amaxa nucleofector system and the amaxa electroporation transfection reagent VPD-1005 (Lonza) according to the manufacturer's procedure.

Western blotting

CAD cells were seeded 1,000,000 in 25 cm flasks. The following day, cells were transfected with 4 µg of GFP-480-68Q or GFP-480-17Q as described above. After 48 hours, cells were washed in D-PBS and lysed in 0.5% Triton X-100, 0.5% sodium deoxycholate, 100 mM NaCl, 10 mM Tris-HCl (pH 8). After a short centrifugation (3000 g for 5 minutes), 40 µg of cell lysate were resolved by SDS-PAGE either on a 7.5% acrylamide gel and western blot with MAB2166 (Millipore) anti-huntingtin antibody (1:5000) or on a 12% acrylamide gel and probed with antibodies against cleaved caspase 3 [(Asp175) (5A1E); Millipore] and cleaved PARP [(Asp214) (7C9); Millipore], as markers of apoptosis. Blots were stripped and re-probed with mouse anti-tubulin (mouse monoclonal antibody, 1:5000) (Sigma). HRP-conjugated secondary antibodies and ECL TM reagents from Amersham (GE Healthcare) were used for detection.

Flow cytometry

CAD cells were transfected separately with GFP-480-68Q, GFP-480-17Q and mCherry constructs in 25 cm flasks as described above.

For co-culture experiments, 1 day after transfection, mCherry-expressing CAD cells were co-cultured with cells expressing either GFP-480-68Q or GFP-480-17Q at a ratio 1:1 in 35 mm dishes. After 24 hours co-culture cells were scraped in D-PBS plus 1% FBS, passed through 40 µm nylon cell strainers and fixed in 2% paraformaldehyde overnight prior to flow cytometry analysis (BD Biosciences LSRFortessa cell analyzer). Each experiment was performed in triplicate and repeated three times. 10,000 cells were counted each time.

GFP-480-68Q- or GFP-480-17Q-expressing cells were also plated on 0.4 µm filters (Costar) placed on top of mCherry-expressing cells in order to inhibit cell-cell contact. After co-culture for 24 hours, the filters were removed and the mCherry-expressing cells were analyzed by flow cytometry as described above.

In order to test supernatant involvement in transfer, CAD cells were transfected separately with GFP-480-68Q and GFP-480-17Q. After 24 hours, cells were gently washed with D-PBS and fresh medium was added for an additional 24 hours. Then, the medium from GFP-480-Q68 or GFP-480-Q17 CADs was used to culture mCherry-expressing CAD (transfected the day before). After 24 hours incubation, mCherry-expressing cells were analyzed by flow cytometry as described above.

For cell viability assay, one day after transfecting cells with GFP-480-17Q or GFP-480-68Q, cells were plated on Ibidi dishes. After 48 hours post-transfection, the supernatant was kept for flow cytometry analysis. Both adherent and detached cells were stained with propidium iodide following manufacturer's instructions (Ebiosciences). The supernatant and adherent cells were analyzed separately by flow cytometry (CyAn ADP Analyzer, Beckman Coulter, Inc.). Experiments have been carried out at least three times.

CGN co-cultures

CGNs transfected with mCherry were mixed with GFP-480-Q68-transfected neurons at a ratio 1.5:1 immediately after nucleofection and plated on coverslips as described above.

Immunofluorescence

At the indicated times post-transfection, cells were washed in D-PBS (Dulbecco's phosphate-buffered saline; Gibco) and fixed in 4% paraformaldehyde (Electron Microscopy Sciences). The cells were permeabilized with 0.1% Triton X-100 and labeled with mouse anti-huntingtin antibody (1:300, for 18 hours at 4°C; MAB2166; Millipore). The Alexa Fluor[®] 633 secondary antibody was purchased from Invitrogen. When indicated, CAD cells were stained with HCS *CellMask*[™] Blue (1:10,000 for 20 minutes at room temperature; Invitrogen), wheat germ agglutinin (WGA)-Rhodamine or WGA-Alexa-Fluor[®]-350 conjugate (1:300 for 20 minutes at room temperature; Invitrogen). For vimentin staining, after 24 hours and 36 hours GFP-480-68Q transfection, cells were washed with PBS and briefly fixed using 80% cold methanol (Sigma). Cells were permeabilized with 0.05% saponin (Merck Millipore) and 2% BSA (Sigma) in PBS for 1 hour at room temperature. Then cells were immunostained using anti-vimentin antibody (D21H3, Cell Signaling) followed by secondary antibody coupled to Alexa Fluor 546 (Invitrogen). For labeling with the long-chain dialkylcarboyanines lipophilic dye, Dil, cells were incubated at the indicated time post-transfection for 30 minutes at 37°C, washed and chased at 37°C in buffer medium for 1 hour at 37°C (1:3000; Invitrogen) before fixation with PFA.

CGNs were also stained with DAPI (1:5000; Sigma). The cells were washed and mounted with Aqua-Poly/Mount (Polysciences).

Images were acquired with a wide-field microscope (Zeiss Axiovert 200M) controlled by Axiovision software. All Z-stacks were acquired with Z-steps of 0.4 µm. For CAD cells, the HCS *CellMask*[™] staining was used to set the autofocus module, providing single focal plane images. When indicated, random

mosaics of (3×3 fields) were obtained using a 63×objective Plan-Apochromat objective (1.4 NA). Representative tiles are presented.

Images of CAD cells used for 3D reconstruction and TNTs detection were acquired with an optimal Z-step of 0.25 µm covering the whole cellular volume.

TNTs (Tunneling nanotubes) detection

CAD cells were transfected with the indicated constructs in 25 cm flasks. The following day or 12 hours post-transfection, cells were plated on µ-Dish^{35 mm, high} (Ibidi[®]) and fixed at the indicated time with a solution of 2% paraformaldehyde, 0.05% glutaraldehyde and 0.2 M HEPES in D-PBS for 20 minutes, followed by a second 20 minutes fixation with 4% paraformaldehyde and 0.2 M HEPES in D-PBS. Then cells were gently washed in D-PBS and stained as indicated.

Image processing and quantification

Raw data were processed with Axiovision 4.8 software. The auto-scaling (min/max) of signal detection was applied to all images. When indicated, images were deconvolved and three-dimensional reconstructions were performed using Huygens Professional software (V.4.3. 0p7).

To quantify the percentage of CAD cells with GFP-480-68Q aggregates and to evaluate the number of TNT-connected cells, a manual analysis was performed as previously shown (Gousset et al., 2009). Experiments were made in triplicate and repeated three times.

FACS raw data were analyzed by Kaluza[®] Flow Cytometry software (Beckman Coulter, Inc.).

To quantify the number of GFP-480-68Q aggregates in CAD cell and their size (expressed as percent of the cell volume) at the different time points, a computer batch run was performed with Huygens Professional Software (V.4.3. 0p7 – Scientific Volume Imaging B.V.) using the Object Analyser Module (V.4.3. 0p7 – Scientific Volume Imaging B.V.). The statistic tests (Tukey's multiple comparisons tests) have been performed with Prism software (V6 – GraphPad).

Image analysis using Acapella[™] software

In order to evaluate and quantify the transfer of polyQ aggregates from donor (GFP-480-Q68 transfected) to acceptor (mCherry transfected) CGN in co-culture experiments, we used the Acapella[™] image analysis software (version 2.3 – Perkin Elmer Technologies) provided by the Plate-forme d'Imagerie Dynamique (Institut Pasteur) that allowed detecting in an automated manner Htt aggregates (GFP-tagged) in mCherry-labeled neurons.

The script is subdivided in four object segmentation subroutines and required the setting of several input parameters:

Segmentation of the nuclei in channel 305 (DAPI staining; detection of nuclei).

Automated detection of the cell body of acceptor cells (mCherry-labeled neurons) in the channels 305 (nuclei, DAPI staining) and 546 (mCherry signal) by applying a mask that allowed the selection of the cell bodies labeled only in both channels (DAPI/mCherry overlap).

Neurite detection. Starting from the selected cell bodies, the application of a specific module of the Acapella software (neurite detection) allowed to automatically draw the neuritic arborization corresponding to each cell body that, at this stage, appeared as 'lines' in the 546 channel (mCherry signal). Then, to gain the thickness, a dilatation filter (radius=3) was applied to the neuritic arbors.

Spot and small object detection. In order to detect Htt aggregates two different algorithms were applied: spots and small object detection in both 488 (GFP-480-68Q signal) and 633 (anti-Htt MAB2166) channels. While the spot detection is based on a local intensity analysis with each spot corresponding to a local intensity maximum, the small object detection takes into account not only the global intensity but also shape and size. Spot and small objects were scored as 'within neurite' only in presence of a shape overlap with the neurite of at least 70%. We consider only spot and small object that were positive in both 488 (GFP-480-68Q signal) and 633 (anti-Htt MAB2166) channels (based on a shape overlap).

The input parameters were optimized with feasibility studies in collaboration with image analysis experts at Plate-forme d'Imagerie Dynamique (Institut Pasteur) and prevented the automated detection of non-neuronal cells (e.g. astrocytes). Different versions of the script corresponding to parameter adjustment were validated and included the use of GFP vector transfected neurons (versus GFP-480-68Q) as negative control.

Acknowledgements

We are grateful to Dr Sandrine Humbert (Institut Curie, UMR 146 du CNRS, Centre Universitaire Orsay, France) for the GFP-HttQ68 and GFP-HttQ17 constructs and for discussions. We thank Emmanuelle Perret (Plate-Forme d'Imagerie Dynamique at Pasteur Institute) for assistance with microscopy; Mickael Machicoane for kindly providing anti-vimentin antibody; Dr Marc Laverrière for his help in cell death flow cytometry assay; and all the members of the Zurzolo Lab for helpful discussions and Dr Karine Gousset for critical reading of the manuscript.

Author contributions

C.Z. conceived and directed the research. M.C. designed and performed the majority of the experiments and analyzed the data. S.A. helped in designing and performing the experiments of aggregates characterization and transfer in TNTs. L.M. set and helped performing the FACS experiments and analysis of the data. Z.C. helped with the transfer assay in primary neuronal cultures. A.D. and P.R. provided the know-how for the quantitative image analysis. M.C. and C.Z. wrote the paper. All authors discussed the results.

Funding

This work was supported by the European Union FP7 [Priority, grant number 222887 to C.Z.]; the Agence Nationale de la Recherche (ANR) [grant numbers ANR-09-BLAN-0122 and ANR-09-NEUR-002-03 to C.Z.]; and the Pasteur-Weizmann Foundation (2010–2012) to C.Z. M.C. and SA were supported by PhD fellowships from the Ministère de l'Éducation Nationale et de la Recherche; M.C. received a 4th year PhD fellowship from the Fondation pour la Recherche Médicale.

Supplementary material available online at

<http://jcs.biologists.org/lookup/suppl/doi:10.1242/jcs.126086/-/DC1>

References

- Abounit, S. and Zurzolo, C. (2012). Wiring through tunneling nanotubes—from electrical signals to organelle transfer. *J. Cell Sci.* **125**, 1089–1098.
- Angot, E., Steiner, J. A., Lema Tomé, C. M., Ekström, P., Mattsson, B., Björklund, A. and Brundin, P. (2012). Alpha-synuclein cell-to-cell transfer and seeding in grafted dopaminergic neurons in vivo. *PLoS ONE* **7**, e39465.
- Björkoy, G., Lamark, T., Brech, A., Outzen, H., Perander, M., Øvervatn, A., Stenmark, H. and Johansen, T. (2005). p62/SQSTM1 forms protein aggregates degraded by autophagy and has a protective effect on huntingtin-induced cell death. *J. Cell Biol.* **171**, 603–614.
- Brundin, P., Melki, R. and Kopito, R. (2010). Prion-like transmission of protein aggregates in neurodegenerative diseases. *Nat. Rev. Mol. Cell Biol.* **11**, 301–307.
- Carrell, R. W. and Lomas, D. A. (1997). Conformational disease. *Lancet* **350**, 134–138.
- Costanzo, M. and Zurzolo, C. (2013). The cell biology of prion-like spread of protein aggregates: mechanisms and implication in neurodegeneration. *Biochem. J.* **452**, 1–17.
- Cronier, S., Laude, H. and Peyrin, J.-M. (2004). Prions can infect primary cultured neurons and astrocytes and promote neuronal cell death. *Proc. Natl. Acad. Sci. USA* **101**, 12271–12276.
- Danzer, K. M., Krebs, S. K., Wolff, M., Birk, G. and Hengerer, B. (2009). Seeding induced by alpha-synuclein oligomers provides evidence for spreading of alpha-synuclein pathology. *J. Neurochem.* **111**, 192–203.
- Davies, S. W., Turmaine, M., Cozens, B. A., DiFiglia, M., Sharp, A. H., Ross, C. A., Scherzinger, E., Wanker, E. E., Mangiarini, L. and Bates, G. P. (1997). Formation of neuronal intranuclear inclusions underlies the neurological dysfunction in mice transgenic for the HD mutation. *Cell* **90**, 537–548.
- DiFiglia, M., Sapp, E., Chase, K. O., Davies, S. W., Bates, G. P., Vonsattel, J. P. and Aronin, N. (1997). Aggregation of huntingtin in neuronal intranuclear inclusions and dystrophic neurites in brain. *Science* **277**, 1990–1993.
- Eugenin, E. A., Gaskill, P. J. and Berman, J. W. (2009). Tunneling nanotubes (TNT) are induced by HIV-infection of macrophages: a potential mechanism for intercellular HIV trafficking. *Cell. Immunol.* **254**, 142–148.
- Frost, B., Jacks, R. L. and Diamond, M. I. (2009). Propagation of tau misfolding from the outside to the inside of a cell. *J. Biol. Chem.* **284**, 12845–12852.
- Gousset, K., Schiff, E., Langevin, C., Marijanovic, Z., Caputo, A., Browman, D. T., Chenouard, N., de Chaumont, F., Martino, A., Enninga, J. et al. (2009). Prions hijack tunnelling nanotubes for intercellular spread. *Nat. Cell Biol.* **11**, 328–336.
- Guo, J. L. and Lee, V. M.-Y. (2011). Seeding of normal Tau by pathological Tau conformers drives pathogenesis of Alzheimer-like tangles. *J. Biol. Chem.* **286**, 15317–15331.
- Hansen, C., Angot, E., Bergström, A.-L., Steiner, J. A., Pieri, L., Paul, G., Outeiro, T. F., Melki, R., Kallunki, P., Fog, K. et al. (2011). α -Synuclein propagates from mouse brain to grafted dopaminergic neurons and seeds aggregation in cultured human cells. *J. Clin. Invest.* **121**, 715–725.
- Herrera, F., Tenreiro, S., Miller-Fleming, L. and Outeiro, T. F. (2011). Visualization of cell-to-cell transmission of mutant huntingtin oligomers. *PLoS Curr.* **3**, RRN1210.
- Kegel, K. B., Sapp, E., Yoder, J., Cui, B., Sobin, L., Kim, Y. J., Qin, Z.-H., Hayden, M. R., Aronin, N., Scott, D. L. et al. (2005). Huntingtin associates with acidic phospholipids at the plasma membrane. *J. Biol. Chem.* **280**, 36464–36473.
- Kegel, K. B., Schewkunov, V., Sapp, E., Masso, N., Wanker, E. E., DiFiglia, M. and Goldmann, W. H. (2009). Polyglutamine expansion in huntingtin increases its insertion into lipid bilayers. *Biochem. Biophys. Res. Commun.* **387**, 472–475.
- Kfoury, N., Holmes, B. B., Jiang, H., Holtzman, D. M. and Diamond, M. I. (2012). Trans-cellular propagation of Tau aggregation by fibrillar species. *J. Biol. Chem.* **287**, 19440–19451.
- Konno, M., Hasegawa, T., Baba, T., Miura, E., Sugeno, N., Kikuchi, A., Fiesel, F. C., Sasaki, T., Aoki, M., Itoyama, Y. et al. (2012). Suppression of dynamin GTPase decreases α -synuclein uptake by neuronal and oligodendroglial cells: a potent therapeutic target for synucleinopathy. *Mol. Neurodegener.* **7**, 38.
- Langevin, C., Gousset, K., Costanzo, M., Richard-Le Goff, O. and Zurzolo, C. (2010). Characterization of the role of dendritic cells in prion transfer to primary neurons. *Biochem. J.* **431**, 189–198.
- Lee, S.-J., Desplats, P., Sigurdson, C., Tsigelny, I. and Masliah, E. (2010). Cell-to-cell transmission of non-prion protein aggregates. *Nat. Rev. Neurol.* **6**, 702–706.
- Luk, K. C., Song, C., O'Brien, P., Stieber, A., Branch, J. R., Brunden, K. R., Trojanowski, J. Q. and Lee, V. M.-Y. (2009). Exogenous alpha-synuclein fibrils seed the formation of Lewy body-like intracellular inclusions in cultured cells. *Proc. Natl. Acad. Sci. USA* **106**, 20051–20056.
- Mangiarini, L., Sathasivam, K., Seller, M., Cozens, B., Harper, A., Hetherington, C., Lawton, M., Trotter, Y., Leach, H., Davies, S. W. et al. (1996). Exon 1 of the HD gene with an expanded CAG repeat is sufficient to cause a progressive neurological phenotype in transgenic mice. *Cell* **87**, 493–506.
- Marzo, L., Gousset, K. and Zurzolo, C. (2012). Multifaceted roles of tunneling nanotubes in intercellular communication. *Front. Physiol.* **3**, 72.
- Moreno-Gonzalez, I. and Soto, C. (2011). Misfolded protein aggregates: mechanisms, structures and potential for disease transmission. *Semin. Cell Dev. Biol.* **22**, 482–487.
- Nonaka, T., Watanabe, S. T., Iwatsubo, T. and Hasegawa, M. (2010). Seeded aggregation and toxicity of alpha-synuclein and tau: cellular models of neurodegenerative diseases. *J. Biol. Chem.* **285**, 34885–34898.
- Polymenidou, M. and Cleveland, D. W. (2012). Prion-like spread of protein aggregates in neurodegeneration. *J. Exp. Med.* **209**, 889–893.
- Ren, P.-H., Lauckner, J. E., Kachirskia, I., Heuser, J. E., Melki, R. and Kopito, R. R. (2009). Cytoplasmic penetration and persistent infection of mammalian cells by polyglutamine aggregates. *Nat. Cell Biol.* **11**, 219–225.
- Rosas, H. D., Salat, D. H., Lee, S. Y., Zaleta, A. K., Pappu, V., Fischl, B., Greve, D., Hevelone, N. and Hersch, S. M. (2008). Cerebral cortex and the clinical expression of Huntington's disease: complexity and heterogeneity. *Brain* **131**, 1057–1068.
- Rustom, A., Saffrich, R., Markovic, I., Walther, P. and Gerdes, H.-H. (2004). Nanotubular highways for intercellular organelle transport. *Science* **303**, 1007–1010.
- Saudou, F., Finkbeiner, S., Devys, D. and Greenberg, M. E. (1998). Huntingtin acts in the nucleus to induce apoptosis but death does not correlate with the formation of intranuclear inclusions. *Cell* **95**, 55–66.
- Shin, J.-Y., Fang, Z.-H., Yu, Z.-X., Wang, C.-E., Li, S.-H. and Li, X.-J. (2005). Expression of mutant huntingtin in glial cells contributes to neuronal excitotoxicity. *J. Cell Biol.* **171**, 1001–1012.
- Volpicelli-Daley, L. A., Luk, K. C., Patel, T. P., Tanik, S. A., Riddle, D. M., Stieber, A., Meaney, D. F., Trojanowski, J. Q. and Lee, V. M.-Y. (2011). Exogenous α -synuclein fibrils induce Lewy body pathology leading to synaptic dysfunction and neuron death. *Neuron* **72**, 57–71.
- Vonsattel, J. P. and DiFiglia, M. (1998). Huntington disease. *J. Neuropathol. Exp. Neurol.* **57**, 369–384.
- Wang, Y., Cui, J., Sun, X. and Zhang, Y. (2011). Tunneling-nanotube development in astrocytes depends on p53 activation. *Cell Death Differ.* **18**, 732–742.
- Waxman, E. A. and Giasson, B. I. (2010). A novel, high-efficiency cellular model of fibrillar alpha-synuclein inclusions and the examination of mutations that inhibit amyloid formation. *J. Neurochem.* **113**, 374–388.
- Wu, J. W., Herman, M., Liu, L., Simoes, S., Acker, C. M., Figueroa, H., Steinberg, J. I., Margittai, M., Kaye, R., Zurzolo, C. et al. (2013). Small misfolded Tau species are internalized via bulk endocytosis and anterogradely and retrogradely transported in neurons. *J. Biol. Chem.* **288**, 1856–1870.
- Yang, W., Dunlap, J. R., Andrews, R. B. and Wetzel, R. (2002). Aggregated polyglutamine peptides delivered to nuclei are toxic to mammalian cells. *Hum. Mol. Genet.* **11**, 2905–2917.
- Zala, D., Colin, E., Rangone, H., Liot, G., Humbert, S. and Saudou, F. (2008). Phosphorylation of mutant huntingtin at S421 restores anterograde and retrograde transport in neurons. *Hum. Mol. Genet.* **17**, 3837–3846.
- Zhang, Y. (2011). Tunneling-nanotube: A new way of cell-cell communication. *Commun. Integr. Biol.* **4**, 324–325.